

SWIFT-UVOT-CALDB-05-R02

Date Original Submitted: 7th November 2005

Prepared by: Tracey Poole

Date Revised: 12th March 2007

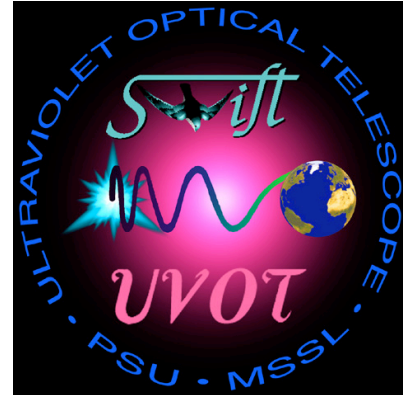
Revision #02

Revised by: Tracey Poole, Alice Breeveld

Pages Changed: All

Comments:

Updated effective area curve for each UVOT filter



SWIFT UVOT CALDB RELEASE NOTE

SWIFT-UVOT-CALDB-05-R02: Effective Area Curves

0. Summary:

This product provides the in-orbit effective area curves for the 7 lenticular filters of the UVOT.

1. Component Files:

| FILE NAME | VALID DATE | RELEASE DATE | VERSION |
|-----------|------------|--------------|---------|
| | | | |
| | | | |
| | | | |

2. Scope of Document:

This document contains a description of the effective area curve calibration analysis performed to produce the effective area curve calibration products for the UVOT calibration database.

3. Changes:

This is the second release of the in-orbit effective area curves, replacing the first release in-orbit calibration data.

This version includes the following changes:

- the predicted effective area curves are made by combining sub-component measurements, rather than the effective area from the ground calibration end-to-end test which turned out to have huge error bars
- the aperture used to measure the in-orbit count rates has changed from 6 arcseconds in the optical and 12 arcsecs in the UV, to 5 arcsecs for all filters
- the coincidence loss correction has been improved
- count rates for some standard stars have changed after reprocessing the data and ironing out exposure time problems
- some individual exposures have been removed. WD0947+857 turned out to be variable.
- the white filter transmission curve was not available for earlier versions.

4. Reason For Update:

An update was undertaken to improve the effective area curve calibration with in-orbit observations of known standard stars.

5. Expected Updates:

Further updates are expected following the addition of further observations in the ultraviolet if more suitable standard stars can be obtained.

6. Caveat Emptor:

The original ground-based effective area curves (SWIFT UVOTA calibration files: 20041116) were calculated incorrectly, therefore a comparison between these in-orbit curves and the ground-based curves in earlier versions of the CALDB is meaningless. For this reason, predicted effective area curves using the UVOT instrument response curves were used as the starting point for calculating the in-orbit effective area curves.

Due to the lack of faint spectroscopic standard stars, especially in the ultraviolet, the effective area curves have been calibrated with very few stars.

7. Data Used:

Observations of 10 Landolt stars, 3 white dwarfs, and 2 Oke standard stars with known UBV magnitudes were used for the optical filter analysis. Observations of 3 faint white dwarf stars with known ultraviolet spectra were used for UV filter analysis. Observations of 4 Landolt stars and 2 white dwarf stars were used for the white filter analysis. Where multiple observations were taken, count rates were calculated for individual exposures and then averaged. Observation details, sorted by observation date, can be seen in Table 1.

| Object Name | Filter | Date | Sequence Number | Mode | Exposure Time (sec) |
|---------------------------|--------|------------|-----------------|------|---------------------|
| WD1121+145 | uvw1 | 21/02/2005 | 55250008 | E | 584.4 |
| Sa104sw-338 & sa104sw-244 | u | 22/02/2005 | 55350004 | I | 1380.5 |
| Sa104sw-338 & sa104sw-244 | v | 22/02/2005 | 55350004 | I | 1626.1 |
| WD1657+343 | uvm2 | 25/02/2005 | 55900001 | E | 699.7 |
| WD1657+343 | uvw1 | 25/02/2005 | 55900002 | E | 570.4 |
| WD1657+343 | uvw2 | 25/02/2005 | 55900001 | E | 729.1 |
| WD1657+343 | v | 25/02/2005 | 55900002 | E | 605.79 |
| WD1121+145 | uvm2 | 04/03/2005 | 55250010 | E | 671.82 |
| WD1121+145 | uvm2 | 04/03/2005 | 55250010 | E | 668.0 |
| WD1121+145 | uvw2 | 04/03/2005 | 55250010 | E | 704.5 |
| Sa101-278 & sa101-l3 | b | 05/03/2005 | 54950011 | I | 1523.7 |
| Sa104sw-338 & sa104sw-244 | b | 06/03/2005 | 55350009 | I | 1155.1 |
| Sa104sw-338 & sa104sw-244 | white | 06/03/2005 | 55350011 | I | 1567.4 |
| PG1525-071B | b | 07/03/2005 | 55750005 | I | 619.0 |
| PG1525-071B | u | 07/03/2005 | 55750003 | I | 1327.2 |
| PG1525-071B | v | 07/03/2005 | 55750001 | I | 1268.8 |
| Sa101-278 & sa101-l3 | b | 09/03/2005 | 54950005 | I | 1210.0 |
| Sa101-278 & sa101-l3 | white | 09/03/2005 | 54950006 | I | 1045.8 |
| Sa98offset2-646 | b | 11/03/2005 | 54700003 | I | 1149.7 |
| Sa104n-443 & sa104n-457 | b | 11/03/2005 | 55400005 | I | 508.2 |
| Sa104ne-367 | b | 11/03/2005 | 55450003 | I | 604.5 |
| Sa95sw-102 | u | 11/03/2005 | 54350005 | I | 569.9 |
| Sa98offset2-646 | u | 11/03/2005 | 54700002 | I | 1251.0 |
| Sa95sw-102 | v | 11/03/2005 | 54350004 | I | 3706.5 |
| Sa98offset2-646 | v | 11/03/2005 | 54700001 | I | 1290.9 |
| WD1657+343 | b | 15/03/2005 | 55900003 | I | 351.0 |
| Sa104n-443 & sa104n-457 | u | 21/03/2005 | 55400012 | I | 2025.3 |
| Sa101-278 & sa101-l3 | v | 26/03/2005 | 54950003 | I | 2661.4 |

| | | | | | |
|-------------------------|-------|------------|----------|---|--------|
| Sa95sw-102 | b | 27/03/2005 | 54350011 | I | 1649.3 |
| Sa104ne-367 | u | 28/03/2005 | 55450005 | I | 868.6 |
| Sa104ne-367 | v | 05/04/2005 | 55450008 | I | 725.9 |
| WD1657+343 | u | 12/04/2005 | 55900024 | I | 633.6 |
| Sa104n-443 & sa104n-457 | v | 19/04/2005 | 55400016 | I | 1128.0 |
| WD1121+145 | white | 10/05/2005 | 55250021 | I | 53.3 |
| WD1657+343 | white | 25/06/2005 | 55900032 | I | 154.9 |
| WD1026+453* | b | 07/07/2005 | 55761006 | I | 63.6 |
| Sa95-42* | b | 07/07/2005 | 55763001 | I | 329.1 |
| G24-9 | b | 07/07/2005 | 55762002 | I | 643.0 |
| WD1026+453* | u | 07/07/2005 | 55761005 | I | 36.0 |
| WD1026+453 | uvm2 | 07/07/2005 | 55761004 | E | 361.6 |
| Sa95-42 | v | 07/07/2005 | 55763002 | I | 501.6 |
| G24-9 | v | 07/07/2005 | 55762001 | I | 1016.5 |
| WD1026+453 | uvw1 | 05/10/2005 | 55761007 | I | 376.3 |
| WD1026+453 | uvw2 | 10/11/2005 | 55761009 | I | 391.6 |
| WD1657+343 | u | 14/01/2006 | 55900035 | I | 82.6 |
| WD1657+343 | white | 14/01/2006 | 55900035 | I | 66.7 |

Table 1 - Table containing the observations used to calculate the in-orbit effective area curves. All of the sequence numbers in column 4 are missing their first three digits of 000. In column 5, I represents Image mode, and E represents Event mode. * indicates that there was considerable TOSSLOSS (http://heasarc.gsfc.nasa.gov/docs/swift/analysis/uvot_digest.html#timing) in one of more of the exposures within the observation; these problem exposures were removed.

8. Description of Analysis:

The first step to calculating the in-orbit effective area curves was to produce the in-orbit instrument response curve using the UVOT ground-based instrument response and in-orbit observations. The in-orbit effective area curves were then calculated using in-orbit instrument response and the ground-based filter transmission curves.

8.1. Ground-Based Instrument Response and Filter Transmission Curves

The ground-based instrument response curve was created by considering the known responses of the UVOT detector and filters in the wavelength region 1600Å to 8000Å. The following were considered when calculating the instrument response:-

1. Quantum efficiency of the photon counting system (D.Q.E)
2. Mirror reflectivity
3. Telescope area (596cm²)

Figure 1 shows the ground-based instrument response curve (dashed line) produced by convolving these sub-component measurements using,

$$\text{Instrument Response} = \text{DQE} \times \text{Mirror Reflectivity}^3 \times 596.$$

Figure 2 shows the ground-based filter transmission curves of each UVOT filter (uvot_caldb_filtertransmission_03.doc).

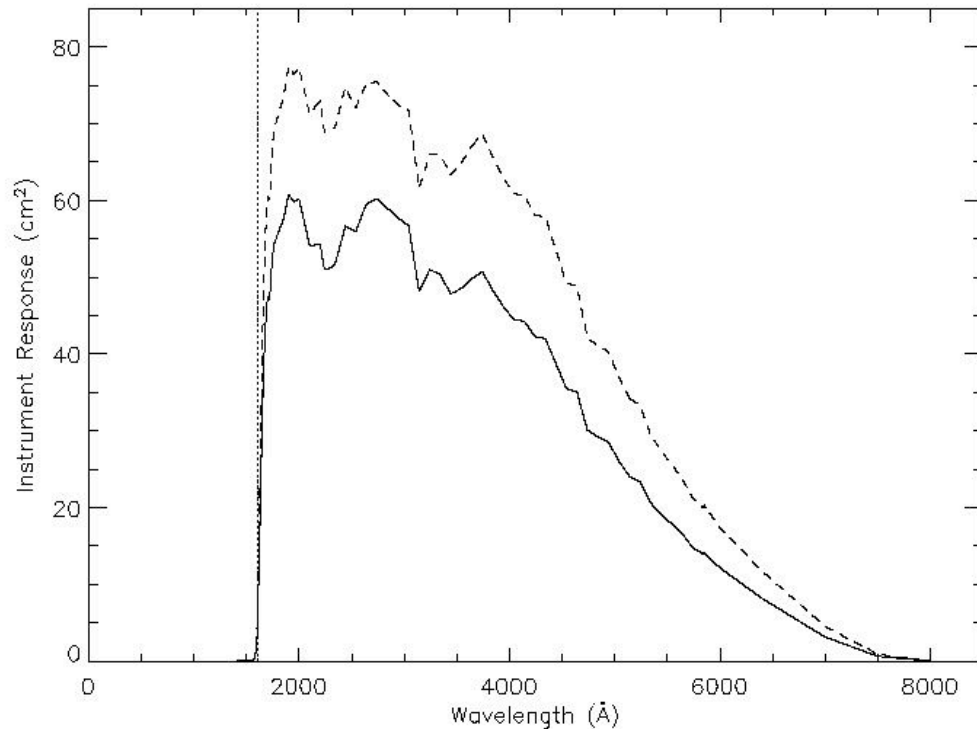


Figure 1 – Instrument response curve. The ground-based curve is the dashed line, and the in-orbit curve is the solid black line.

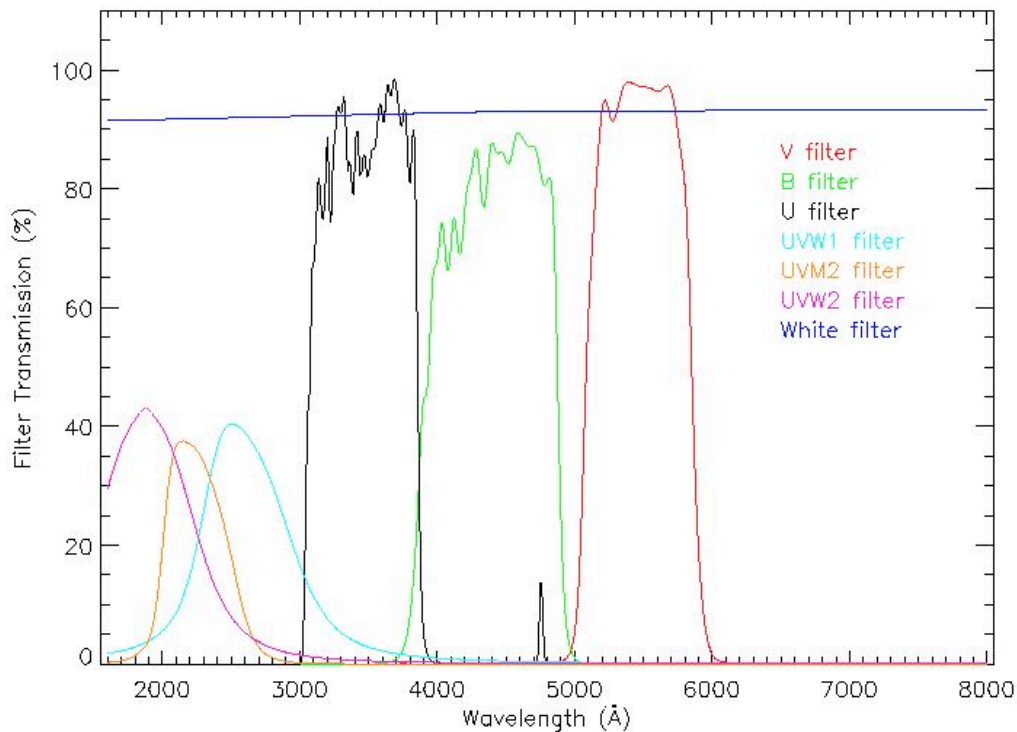


Figure 2 – Ground-based Filter transmission curves for each filter.

8.2. In-orbit Instrument Response Curve

Observations of 10 Landolt stars, 2 Oke standard stars with known UB_V magnitudes, and 3 white dwarfs with known ultraviolet spectra (from HST and IUE) were considered. The spectra of the 2 Oke stars were known from HST data, and the spectra of the 10 Landolt stars were identified by fitting the Landolt star b-v and u-b colours (Landolt 1992, AJ, 104, 340) with known spectra from the Pickles models (<http://www/ifa.hawaii.edu/users/pickles/AJP/hilib.html>).

Raw count rates for each star were extracted using an aperture radius of 10 pixels (5 arcsec) for all filters, and then corrected for coincidence loss. The background region was set to an annulus with an inner radius of 55 pixels (27.5 arcsec), and an outer radius of 70 pixels (35 arcsec). The background extraction method was set depending upon the background level: below a background level of 10 ph/pix a MEAN

background method was used unless there was a bright source in the background region then a CLIPPED MEAN (using a sigma clipping method at 3 sigma) background method was used; above a background level of 10 ph/pix a CLIPPED MEAN background was used.

The raw observed count rate and background count rate for each observation was then corrected with the theoretical coincidence loss equation of,

$$C_{theory} = \frac{-\ln(1 - C_{raw}ft)}{ft(1 - df)},$$

Where C_{theory} is the theoretically coincidence loss corrected count rate, C_{raw} is the raw observed count rate, ft is the frame time (0.0110322s for full frame), and df is the deadtime fraction (0.0157720 for full frame). N.B. This count rate C_{raw} is calculated using an exposure time which is *not* corrected for deadtime. If the count rate is calculated using the deadtime-corrected exposure time recorded in the keyword EXPOSURE, then it must be multiplied by $(1-df)$ to get C_{raw} .

This theoretical coincidence loss is then corrected by multiplying by the in-orbit empirical formula for a 10 pixel (5 arsec) aperture,

$$f(x) = 1.0 + 0.0658568x - 0.0907142x^2 + 0.0285951x^3 + 0.0308063x^4,$$

where $x = C_{raw}ft$.

Finally, the corrected background count rate is subtracted producing a final in-orbit observed count rate of $C_{obs}(i)$, where i is the number of standard stars used.

The observations of sa95-42 were discarded in the b filter due to large TOSS LOSS

(http://heasarc.gsfc.nasa.gov/docs/swift/analysis/uvot_digest.html#timing). There was a large readout streak running through the background region of sa98offset2-646 in the u filter observations so this was also discarded.

The expected count rate of each observed star ($C_{exp}(i)$) for each filter was calculated by convolving the known spectra of the observed stars with the ground-based instrument response curve and the ground-based filter

transmission curve for that filter. The spectra of WD1026+453 had to be extrapolated beyond 5700Å which will affect the V filter. The optical spectrum (3150-8000Å) of WD1121+145 was uncertain therefore this source was removed from the V and B filter analysis. The spectra of SA95-42 and G24-9 range from 3200-8000Å, which will affect all the UV filters and the U filter.

A ratio of observed count rate to expected count rate for each star in each filter was then calculated, and averaged over each filter. These ratio values, along with the central wavelength values of each filter, were then used to produce a *correction curve* in which to correct the ground-based instrument response. The correction curve was produced using a spline fitting routine, with anchors at the wavelength extremes, to fix the curve at 1600Å and 8000Å. Figure 3 shows the correction curve calculated from these ratios. The y-axis error bars show the RMS error of each ratio, and the x-axis error bars give the FWHM of each filter.

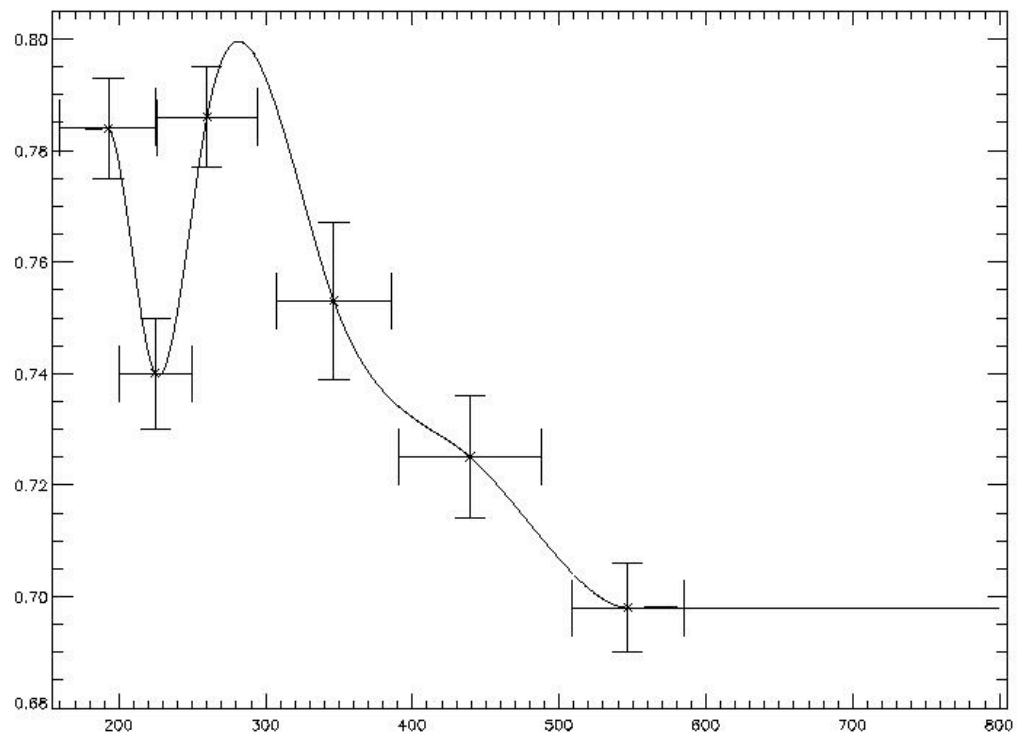


Figure 3 - Correction curve to transform the Instrument response curve from the ground-based measurements to in-orbit measurements. Y-axis error bars are the RMS errors found for each filter ratio, and the x-axis error bars are the FWHM of each filter.

The in-orbit instrument response was then calculated by convolving the ground-based instrument response with the correction curve. Figure 1 plots the in-orbit instrument response (solid black line).

8.3. In-Orbit Effective Area curves

The in-orbit effective area for each filter was then calculated by convolving the in-orbit instrument response with the ground-based filter transmission curves.

When testing these new curves, an extra ratio of 0.88 was need to adjust the white filter data to the correct in-orbit observations. Therefore unlike the other filters the white filter in-orbit effective area curve was calculated using,

$$\textit{White in-orbit effective area} = \textit{In-orbit Instrument Response} \times \textit{Filter Transmission} \times 0.88$$

Figure 4 plots the in-orbit effective area curves (solid lines), and compares them to ground-based effective area curves (dashed lines) that are calculated by convolving the ground-based instrument response curve with the ground-based filter transmission curves for each filter.

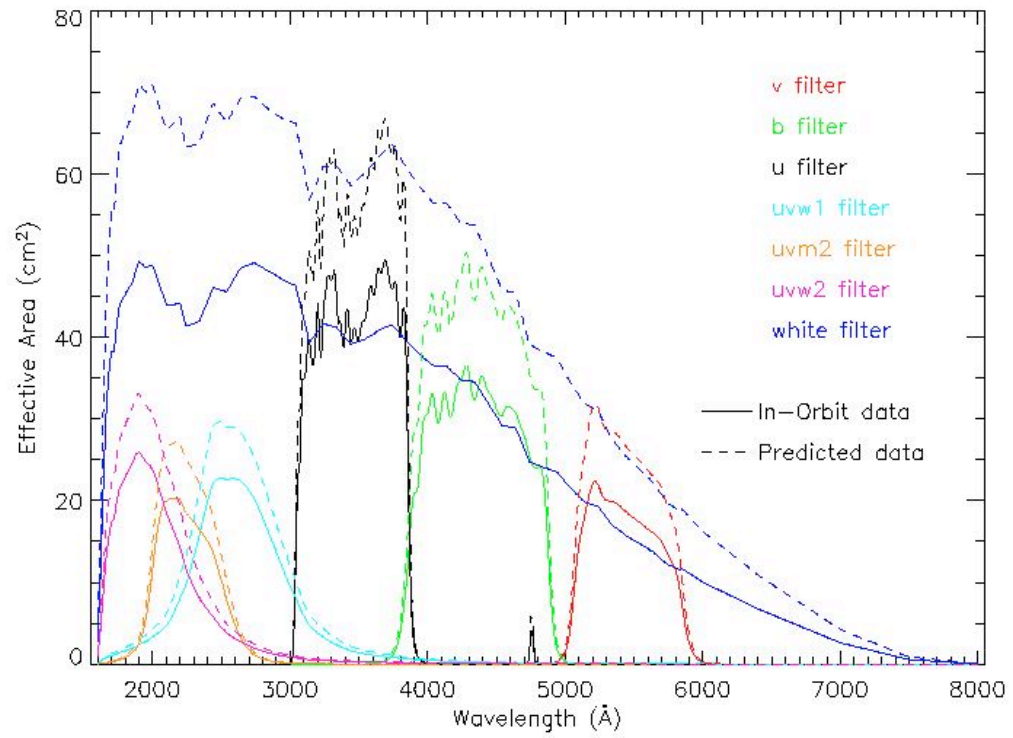


Figure 4 - Comparison between the new in-orbit effective area curves (solid lines) and the ground-based effective area curves (dashed lines), for all the UVOT filters.